A Critical Analysis of Eight-Electromagnet Manipulation Systems: The Role of Electromagnet Configuration on Strength, Isotropy, and Access

Ashkan Pourkand and Jake J. Abbott

***Abstract*—It is known that in the creation of isotropic magnetic manipulation systems using a set of stationary electromagnets, eight electromagnets are necessary to ensure that there are no singularities in the workspace. A variety of eight-electromagnet configurations have been proposed to date. In the first contribution of this letter, we conduct a critical comparison of these proposed configurations, and find that certain configurations are superior in terms of field and torque generation, whereas others are superior in terms of force generation due to the spatial derivative of the field. All of the prior configurations comprise a high degree of symmetry, yet access to the workspace varies widely between designs. In the second contribution of this letter, we propose a new configuration that does not comprise the symmetry seen in prior systems, and also provides more open access to the manipulation workspace than prior systems, yet still exhibits an isotropic workspace with comparable performance to prior systems. We conclude that designers of isotropic eight-electromagnet manipulation systems should not feel obliged to incorporate symmetry into their design.**

***Index Terms*—Dexterous manipulation, haptics and haptic interfaces, medical robots and systems, micro/nano robots, optimization and optimal control.**

I. Introduction

THERE has been a great deal of activity over the past two decades in the design of magnetic manipulation systems that comprise a set of stationary electromagnets surrounding a manipulation workspace. These projects have typically been motivated by the manipulation of microscale objects under a microscope [1], or by the control of medical devices—such as catheters, capsule endoscopes, and microrobots—inside the human body [2]. The OctoMag system [3] was the first to demonstrate the dexterous manipulation of an untethered and unconstrained magnetic dipole, with three-degree-of-freedom (3-DOF) position control and 2-DOF torque control. The OctoMag was so-named because of its use of eight electromagnets, and we now know that eight is the minimum number of stationary electromagnets required to ensure that there are no singularities in the manipulation workspace [4]. Erni *et al.* [5] considered a configuration of eight electromagnets all arranged in a plane, and found that it had singularities in the workspace (unlike the OctoMag). However, a variety of other eight-electromagnet manipulation systems have been developed that have more well-conditioned configurations than a coplanar configuration [6]–[10], yet there has been no published critical comparison of these configurations to each other and to the OctoMag; this is the first contribution of our letter. We show that there is no obvious best system, with a trade-off between torque generation (proportional to the strength of the field), force generation (proportional to the spatial derivative of the field), workspace isotropy, and access to the workspace. We perform a quasistatic analysis, and do not consider system dynamics (e.g., time response, mutual inductance).

We are particularly interested in the use of magnetic manipulation systems for the application of untethered magnetic haptic interfaces, wherein an untethered haptic stylus is equipped with a magnetic tip, and the electromagnets are used to render forces and torques wirelessly to that stylus tip [11], [12]. One of the benefits of the OctoMag configuration over other eight-electromagnet configurations is the relatively open access to its workspace, due to the hemispherical arrangement of the electromagnets, which provides unencumbered access to the workspace from one side. However, with the need to provide access for a hand-held stylus, as well as two cameras to localize the stylus in the workspace, we were forced to consider other electromagnet configurations with even more access to the workspace. We began by simply removing one of the OctoMag's electromagnets (which provided a great deal of access from a new, orthogonal direction), and then moving the other seven electromagnets just enough to accommodate the reintroduction of the eighth (which only slightly compromised access from the original direction). The result is a configuration that we will refer to here simply as the open-asymmetric configuration. We are not making any claims of optimality of this new configuration for any specific cost function, but the configuration has substantially more open access to the workspace than prior configurations while maintaining manipulation capabilities comparable to prior systems (even though the configuration does not exhibit the degree of symmetry seen in prior systems). This is the second contribution of this letter. Although we were motivated by the creation of an untethered magnetic haptic

Manuscript received February 24, 2018; accepted May 30, 2018. Date of publication June 13, 2018; date of current version July 5, 2018. This letter was recommended for publication by Associate Editor Y. Zheng and Editor H. Ding upon evaluation of the reviewers' comments. This work was supported by the National Science Foundation under Grant 1423273. *(Corresponding author: Ashkan Pourkand.)*

A. Pourkand is with the School of Computing and the Robotics Center, University of Utah, Salt Lake City, UT 84112 USA (e-mail: ashkan.pourkand@utah.edu).

J. J. Abbott is with the Department of Mechanical Engineering and the Robotics Center, University of Utah, Salt Lake City, UT 84112 USA (e-mail: jake.abbott@utah.edu).

Digital Object Identifier 10.1109/LRA.2018.2846800

interface, this new configuration also seems promising for medical applications.

II. Background on Magnetic Manipulability

When a magnetic dipole $\boldsymbol{m}\{\mathrm{A{\cdot}m^2}\}$ is placed in a magnetic field $\boldsymbol{b}$ $\{\mathrm{T}\}$, the torque $\boldsymbol{\tau}$ $\{\mathrm{N{\cdot}m}\}$ and force $\boldsymbol{f}$ $\{\mathrm{N}\}$, respectively, generated on the dipole are:

$$\boldsymbol{\tau} = \boldsymbol{m} \times \boldsymbol{b} \tag{1}$$

$$\boldsymbol{f} = (\boldsymbol{m} \cdot \nabla)\boldsymbol{b} \tag{2}$$

where $\nabla = [\frac{\partial}{\partial x}\ \frac{\partial}{\partial y}\ \frac{\partial}{\partial z}]^T$. We can express the dipole and field vectors with respect to their components:

$$\boldsymbol{m} = \begin{bmatrix} m_x \\ m_y \\ m_z \end{bmatrix}, \quad \boldsymbol{b} = \begin{bmatrix} b_x \\ b_y \\ b_z \end{bmatrix} \tag{3}$$

It is well known that the cross-product operation can be expressed using a skew-symmetric matrix, which enables us to express (1) as:

$$\boldsymbol{\tau} = \begin{bmatrix} 0 & -m_z & m_y \\ m_z & 0 & -m_x \\ -m_y & m_x & 0 \end{bmatrix} \begin{bmatrix} b_x \\ b_y \\ b_z \end{bmatrix} \tag{4}$$

In this representation, the roles of the dipole and the field on the resulting torque are separated.

Petruska and Nelson [4] showed that it is similarly possible to separate the roles of the dipole and the spatial derivatives of the field on the resulting force, which enables us to express (2) as:

$$\boldsymbol{f} = \begin{bmatrix} m_x & m_y & m_z & 0 & 0 \\ 0 & m_x & 0 & m_y & m_z \\ -m_z & 0 & m_x & -m_z & m_y \end{bmatrix} \begin{bmatrix} \frac{\partial b_x}{\partial x} \\ \frac{\partial b_x}{\partial y} \\ \frac{\partial b_x}{\partial z} \\ \frac{\partial b_y}{\partial y} \\ \frac{\partial b_y}{\partial z} \end{bmatrix} \tag{5}$$

If the goal is to create an isotropic magnetic manipulation workspace, with full control over the torque and force generated, which should work with the dipole $\boldsymbol{m}$ in all possible orientations, then [4] concludes that we must have at least eight electromagnets in order to independently control the three inputs in (4) and the five inputs in (5). The field can be expressed as the linear combination of the field due to each of the electromagnets:

$$\begin{bmatrix} b_x \\ b_y \\ b_z \end{bmatrix} = \begin{bmatrix} b_{1x} & b_{2x} & \dots & b_{8x} \\ b_{1y} & b_{2y} & & b_{8y} \\ b_{1z} & b_{2z} & & b_{8z} \end{bmatrix} \begin{bmatrix} i_1 \\ i_2 \\ \vdots \\ i_8 \end{bmatrix} \tag{6}$$

and the force can be expressed as the linear combination of the field derivatives due to each of the electromagnets:

$$\begin{bmatrix} \frac{\partial b_x}{\partial x} \\ \frac{\partial b_x}{\partial y} \\ \frac{\partial b_x}{\partial z} \\ \frac{\partial b_y}{\partial y} \\ \frac{\partial b_y}{\partial z} \end{bmatrix} = \begin{bmatrix} \frac{\partial b_{1x}}{\partial x} & \frac{\partial b_{2x}}{\partial x} & & \frac{\partial b_{8x}}{\partial x} \\ \frac{\partial b_{1x}}{\partial y} & \frac{\partial b_{2x}}{\partial y} & & \frac{\partial b_{8x}}{\partial y} \\ \frac{\partial b_{1x}}{\partial z} & \frac{\partial b_{2x}}{\partial z} & \cdots & \frac{\partial b_{8x}}{\partial z} \\ \frac{\partial b_{1y}}{\partial y} & \frac{\partial b_{2y}}{\partial y} & & \frac{\partial b_{8y}}{\partial y} \\ \frac{\partial b_{1y}}{\partial z} & \frac{\partial b_{2y}}{\partial z} & & \frac{\partial b_{8y}}{\partial z} \end{bmatrix} \begin{bmatrix} i_1 \\ i_2 \\ \vdots \\ i_8 \end{bmatrix} \tag{7}$$

The singular values (σ_i) of the 3×8 actuation matrix in (6) and the 5×8 actuation matrix in (7) can be used to quantify the torque-control and force-control authority, respectively, over a magnetic dipole in any possible orientation. This is an improvement over the related methodology of [3], since it no longer requires that the to-be-manipulated magnetic dipole be explicitly considered in the analysis of the system's manipulability.

III. Critical Comparison of Eight-Electromagnet Configurations

In this section, we critically compare four eight-electromagnet configurations used in magnetic manipulation systems (Fig. 1). The first two configurations (square-antiprism and OctoMag) have been highly utilized in the literature, and the third configuration has been utilized in a commercial system (Magnetecs CGCI). All three of these systems comprise a high degree of symmetry. In the fourth system, we propose a new configuration that substantially violates an assumption of symmetry, and we find that its performance is comparable to the other three. In each configuration, we quantify performance of the workspace in terms of torque- and force-generation capability (both magnitude and isotropy) and we quantify accessibility of the workspace as a set of unoccupied solid angles. In each of the configurations considered, we assume, in order of priority: (1) that all electromagnets are cylinders of the same dimensions, with outer diameter D_o; (2) that the axes of the electromagnets all intersect at a common point, which is assumed to be the center of the manipulation workspace; (3) that all electromagnets are the same distance from that common point; (4) and that all electromagnets are as close as possible to the common point, such that a collision between electromagnets has occurred. In Section III-A we describe each of the configurations, in Section III-B we describe the methodology used in our comparison, and in Section III-C we provide the results of our comparison.

A. Electromagnet Configurations

1) Square Antiprism: With the knowledge that eight linearly independent magnetic fields are required for full manipulability, it is natural to attempt to place each of the eight electromagnets as far away from each other as possible so that their field contributions are distinct, while still keeping them close to the

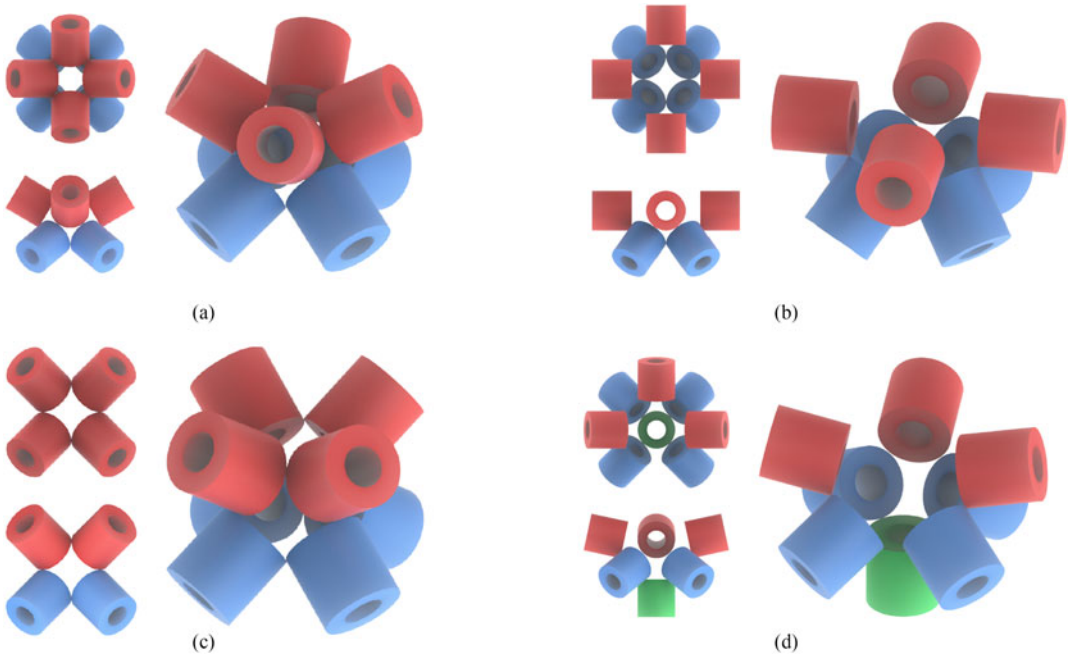

Fig. 1. The four eight-electromagnet configurations considered. The upper set is indicated in red, and the lower set is indicated in blue. In the open-asymmetric configuration, one of the upper magnets is removed, and a new magnet indicated in green is placed between the electromagnets in the lower set. (a) Square-antiprism configuration. (b) OctoMag configuration. (c) Magnetecs-CGCI configuration. (d) Open-asymmetric configuration.

manipulation workspace. This problem is very related to that of Thomson [13], who considered the equilibrium spacing of electrons in an atom as they are attracted to the nucleus but repelled from each other. For our problem, this is equivalent to placing the electromagnets on and normal to a sphere, and as far as possible from each other on that sphere. Thomson's method proposes the *square antiprism* arrangement as the solution to this problem for eight objects. In the square antiprism, two square parallel plates, separated by a distance equal to the sphere's radius, are arranged with a common central normal axis, and one of them is rotated 45° about that axis; the solution is then the eight corners of the plates. Figure 1(a) shows electromagnets in this configuration, which is created as follows: each electromagnet in the upper set[1] is rotated 60° from the common axis of symmetry; each electromagnet in the lower set is rotated 60° from the common axis of symmetry; and the lower set is rotated 45° about its axis of symmetry, relative to the upper set. In this arrangement, if the electromagnets are allowed to be placed as close as possible to the center of the workspace before self-collision, the innermost surfaces of the electromagnets are located at a distance $1.31D_o$ from the center of the workspace. Access to the workspace is relatively restricted, with two 48° solid angles and eight 16° solid angles that are all isolated from one another. This (approximate) configuration has been utilized in previous systems [7]–[9], although the connection to the square antiprism has not been discussed previously.

2) OctoMag: Kummer *et al.* [3] presented a configuration known as the "OctoMag". Figure 1(b) shows electromagnets in this configuration, which is created as follows: each electromagnet in the upper set is rotated 90° from the common axis of symmetry, so that they lie in a common plane; each electromagnet in the lower set is rotated 45° from the common axis of symmetry; and the lower set is rotated 45° about its axis of symmetry, relative to the upper set. In this arrangement, the electromagnets are arranged on a hemisphere, and if the electromagnets are allowed to be placed as close as possible to the center of the workspace before self-collision, the innermost surfaces of the electromagnets are located at a distance $1.73D_o$ from the center of the workspace. Access to the workspace is quite open from one side, with a 120° solid angle and four adjoining 10° solid angles, and with an additional five 30° solid angles that are isolated from one another and from the large access opening. As described in [3], the OctoMag design was the result of a constrained optimization to maximize the worst-case force generation, which is equivalent to maximizing the value of σ_5 in the actuation matrix of (7), using the rationale that forces are more important than torques for the control of levitating untethered devices that are free to rotate and align with the applied field. Others have proposed small modifications to the OctoMag configuration [6], including a small deviation of its symmetry (see [14], Fig. 3).

3) Magnetecs CGCI: Magnetecs (Inglewood, California) has created a system that they call the Catheter Guidance Control and Imaging (CGCI) system. Based on photos and illustrations available online, we estimate the configuration as depicted in Figure 1(c), which is created as follows: each electromagnet in the upper set is rotated 54.7° from the common axis of symmetry; each electromagnet in the lower set is rotated 54.7° from the common axis of symmetry; and the lower set is not rotated

[1]Throughout this section we refer to the "upper" and "lower" sets of electromagnets in reference to Fig. 1, but there is no inherent sense of up or down in any of the analysis in this letter.

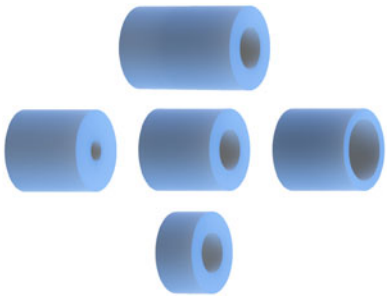

Fig. 2. The dimensions of electromagnets considered, with $L/D_o = \{0.5, 1, 1.5\}$ and $D_i/D_o = \{0.25, 0.5, 0.75\}$, shown in the same arrangement as the results in Table I.

relative to the upper set. In this arrangement, if the electromagnets are allowed to be placed as close as possible to the center of the workspace before self-collision, the innermost surfaces of the electromagnets are located at a distance $1.41D_o$ from the center of the workspace. Access to the workspace is the most restricted of the configurations considered here, with six 40° solid angles that are all isolated from one another.

4) Open-Asymmetric Configuration: The proposed open-asymmetric configuration that we consider here is depicted in Figure 1(d), which is created as follows: each electromagnet in the upper set is rotated 80° from the common axis of symmetry; each electromagnet in the lower set is rotated 60° from the common axis of symmetry; the lower set is rotated 45° about its axis of symmetry, relative to the upper set; and one of the electromagnets from the upper set is removed and relocated to correspond with the axis of symmetry of the lower set. In this arrangement, if the electromagnets are allowed to be placed as close as possible to the center of the workspace before self-collision, the innermost surfaces of the electromagnets are located at a distance $1.73D_o$ from the center of the workspace. This is the same relative distance as the OcoMag system by design; we chose the angles of the electromagnets to maintain that distance, as well as the angular distance between neighboring magnets of 60°. It is nearly as easy to access the workspace from above as with the OctoMag configuration, but it is also substantially easier to access the workspace from one side, creating a very open configuration that can be described as a 100° solid angle, an adjoining 60° solid angle, and four adjoining 30° solid angles, with an additional four 18° solid angles that are isolated from one another and from the large access opening. Unlike each of the other three configurations, this proposed configuration does not comprise a high degree of symmetry. In fact, another way of thinking about the construction of this configuration is to create a symmetric nine-electromagnet system similar in spirit to the OctoMag, and then simply remove one of the electromagnets.

B. Methodology for Numerical Comparison

In this study, for each of the four configurations, we consider five different electromagnets of varying lengths and inner diameters (see Fig. 2) so as to not bias our comparison in favor of one particular electromagnet design. For each of these five electromagnets, we created a lookup table by calculating the field in a cubic workspace of side length $4D_o$ centered directly adjacent to the innermost surface of the electromagnet, with a discretization of 1600 points in each dimension, for a total of 4.096×10^9 points. This high number was chosen to avoid any potential errors due to discretization. The magnetic field at each point is calculated by the Biot-Savart law integrated over the volume of the cylindrical coil, which is defined with respect to a Cartesian coordinate systems attached to the coil's innermost face with x defined as the main axis of the coil:

$$\boldsymbol{b}(\boldsymbol{p}) = \frac{\mu_0 J}{4\pi} \int_{x=0}^{x=L} \int_{r=\frac{D_i}{2}}^{r=\frac{D_o}{2}} \int_{\theta=0}^{\theta=2\pi} \boldsymbol{\beta}(\boldsymbol{p}, x, r, \theta) d\theta dr dx \quad (8a)$$

$$\boldsymbol{\beta}(\boldsymbol{p}, x, r, \theta) = \frac{\begin{bmatrix} 0 \\ r\cos(\theta) \\ -r\sin(\theta) \end{bmatrix} \times \left(\boldsymbol{p} - \begin{bmatrix} x \\ r\sin(\theta) \\ r\cos(\theta) \end{bmatrix} \right)}{\left\| \boldsymbol{p} - \begin{bmatrix} x \\ r\sin(\theta) \\ r\cos(\theta) \end{bmatrix} \right\|^3} \quad (8b)$$

where $\boldsymbol{p}$ $\{\mathrm{m}\}$ is the point at which we are calculating the magnetic field $\boldsymbol{b}$, $\mu_0 = 4\pi \times 10^{-7}$ $\mathrm{T{\cdot}m{\cdot}A^{-1}}$ is the permeability of free space, J $\{\mathrm{A{\cdot}m^{-2}}\}$ is the current density, L $\{\mathrm{m}\}$ is the length of the coil, and D_i $\{\mathrm{m}\}$ and D_o $\{\mathrm{m}\}$ are the inner and outer diameters of the coil, respectively. In our simulation, we exclusively considered $D_o = 0.1$ m and $J = 10^{-6}$ $\mathrm{A{\cdot}m^{-2}}$.

When evaluating the manipulability of each configuration, we considered a cubic workspace of side length $0.5D_o$, centered at the common intersection point of the electromagnets' axes. We consider the center of the cubic workspace, as well as the corners of the cube and the centers of each of its edges and faces, for a total of 27 points throughout the workspace. At each of these points, we compute the singular values of the 3×8 actuation matrix in (6) and the 5×8 actuation matrix in (7). From those values, we find the smallest singular values, σ_3 and σ_5, respectively, which we would like to be as large as possible to maximize the strength of the system in the conservative worst-case. We also compute the condition numbers of the actuation matrices, $\kappa = \sigma_3/\sigma_1$ and $\kappa = \sigma_5/\sigma_1$, respectively, which we would like to be as close to unity as possible to maximize isotropy. We compute each of the above metrics at each of the 27 points throughout the workspace.

C. Results

Table I shows the results of the comparison between the four configurations. For each of the 3×8 actuation matrix in (6) and the 5×8 actuation matrix in (7), we report the condition number and smallest singular value at the center of the workspace, as well as their maximum and minimum values across all 27 points in the workspace. Each cell in the table contains five values, arranged to correspond to the electromagnets as depicted in Fig. 2. In our opinion, $\sigma_{3,\min}$ and $\sigma_{5,\min}$ are the most important parameters to consider, since they represent the location in the workspace where control authority is the worst, thus they are conservative metrics of manipulation capability. Note: the numerical values reported for the singular values are for a system

TABLE I
RESULTS OF THE COMPARISON BETWEEN THE FOUR ELECTROMAGNET CONFIGURATIONS OF FIG. 1, FOR THE FIVE ELECTROMAGNET GEOMETRIES OF FIG. 2. FOR EACH OF THE METRICS, THE SUBSCRIPT O INDICATES THE VALUE AT THE CENTER OF THE WORKSPACE, AND THE SUBSCRIPTS $\max$ AND $\min$ INDICATE THE MAXIMUM AND MINIMUM VALUES, RESPECTIVELY, FOUND ACROSS THE 27 POINTS IN THE WORKSPACE.

		Square-Antiprism			OctoMag			Magnetecs CGCI			Open-Asymmetric		
Field (Torque)	κ_{max}		0.71			0.67			0.72			0.84	
		0.73	0.72	0.70	0.70	0.67	0.65	0.72	0.72	0.73	0.81	0.84	0.85
			0.71			0.68			0.71			0.84	
	κ_O		0.70			0.63			0.67			0.80	
		0.71	0.70	0.70	0.66	0.63	0.61	0.65	0.66	0.69	0.76	0.79	0.81
			0.70			0.64			0.65			0.79	
	κ_{min}		0.69			0.59			0.59			0.72	
		0.69	0.68	0.68	0.62	0.59	0.58	0.54	0.58	0.64	0.67	0.72	0.75
			0.68			0.60			0.56			0.71	
	$\sigma_{3,max}$		2.1e-06			1.6e-06			2.1e-06			1.9e-06	
		2.4e-06	1.9e-06	7.9e-07	1.8e-06	1.5e-06	6.2e-07	2.2e-06	1.9e-06	7.9e-07	2.0e-06	1.7e-06	7.4e-07
			1.4e-06			1.1e-06			1.4e-06			1.2e-06	
	$\sigma_{3,O}$		2.1e-06			1.6e-06			2.0e-06			1.7e-06	
		2.3e-06	1.9e-06	7.8e-07	1.7e-06	1.4e-06	6.1e-07	2.1e-06	1.8e-06	7.7e-07	1.7e-06	1.5e-06	6.7e-07
			1.4e-06			1.0e-06			1.3e-06			1.1e-06	
	$\sigma_{3,min}$		2.0e-06			1.6e-06			2.0e-06			1.5e-06	
		2.2e-06	1.8e-06	7.6e-07	1.7e-06	1.4e-06	6.0e-07	2.0e-06	1.8e-06	7.7e-07	1.5e-06	1.4e-06	6.0e-07
			1.3e-06			1.0e-06			1.3e-06			9.8e-07	
Field Spatial Derivative (Force)	κ_{max}		0.33			0.33			0.11			0.65	
		0.35	0.33	0.31	0.33	0.33	0.33	0.13	0.11	0.09	0.62	0.65	0.67
			0.32			0.33			0.10			0.66	
	κ_O		0.30			0.33			0.07			0.56	
		0.31	0.30	0.30	0.33	0.33	0.33	0.10	0.07	0.03	0.54	0.56	0.57
			0.30			0.33			0.06			0.56	
	κ_{min}		0.21			0.32			0.02			0.41	
		0.18	0.21	0.24	0.32	0.32	0.33	0.06	0.02	0.02	0.38	0.40	0.45
			0.22			0.32			0.02			0.41	
	$\sigma_{5,max}$		7.6e-06			9.0e-06			3.4e-06			1.0e-05	
		1.1e-05	6.9e-06	2.4e-06	1.1e-05	8.3e-06	3.1e-06	4.8e-06	3.1e-06	1.0e-06	1.3e-05	9.1e0-6	3.4e-06
			5.0e-06			6.1e-06			2.3e-06			6.8e-06	
	$\sigma_{5,O}$		7.6e-06			8.8e-06			2.6e-06			8.4e-06	
		1.1e-05	6.9e-06	2.4e-06	1.1e-05	8.0e-06	3.0e-06	4.1e-06	2.3e-06	3.0e-07	1.0e-05	7.7e-06	3.0e-06
			5.0e-06			5.9e-06			1.4e-06			5.7e-06	
	$\sigma_{5,min}$		5.5e-06			8.7e-06			7.3e-07			7.1e-06	
		6.9e-06	5.0e-06	2.0e-06	1.1e-05	8.0e-06	3.0e-06	2.3e-06	7.2e-07	1.8e-07	8.7e-06	6.5e-06	2.6e-06
			3.8e-06			5.9e-06			4.5e-07			4.8e-06	
Access solid angles		$44^\circ \times 2 + 16^\circ \times 8$			$(120^\circ + 10^\circ \times 4) + 30^\circ \times 5$			$40^\circ \times 6$			$(100^\circ + 60^\circ + 30^\circ \times 4) + 18^\circ \times 4$		

with a single (arbitrary) D_o and J, so the absolute values are only meaningful for that specific case, so these values should only be used to make relative comparisons between configurations. The condition numbers, however, are invariant to the values of D_o and J chosen.

As expected, larger electromagnets lead to higher values in terms of both field (torque) and field derivative (force). However, we find that the condition number is insensitive to the size of the electromagnets. We also find that, with few exceptions, the results of a relative comparison between configurations is insensitive to the size of the electromagnets.

In terms of field-generation capability, which corresponds to torque-generation capability, we find that the square-antiprism and Magnetecs-CGCI configurations are the strongest, and the OctoMag and open-asymmetric configurations are the weakest. However, the weaker configurations are only $\sim$22% weaker that the strongest configurations (using $\sigma_{3,\min}$). We find that the open-asymmetric configuration is the best in terms of workspace conditioning ($\kappa_{\min}$), but the correct interpretation of this result is that the system is more-equally weak. We find that the square-antiprism configuration is the second-best in terms of workspace conditioning, and the correct interpretation of this result is that the system is more-equally strong.

In terms of the generation of a spatial derivative in the field, which corresponds to force-generation capability, we find that the OctoMag configuration is the strongest, followed by the open-asymmetric configuration ($\sim$81% the strength of OctoMag), then the square-antiprism configuration ($\sim$63% the

strength of OctoMag), with the Magnetecs-CGCI configuration being the weakest ($\sim$9% the strength of OctoMag), all using $\sigma_{5,\min}$. We find that the open-asymmetric configuration is best in terms of workspace conditioning ($\kappa_{\min}$), and the correct interpretation of this result is that the system is more-equally moderate. We find that the Magnetecs-CGCI configuration is by far the worst in terms of workspace conditioning, which when combined with the results for $\sigma_{5,\min}$ reveals that there are locations in that system's workspace in which control authority (in terms of force) is substantially reduced.

IV. Discussion

From the preceding results, it is clear that there is no clear best system overall. We must be aware of the intended application. For systems in which force generation is not important (e.g., using torque-based control of helical swimming microrobots), the square-antiprism and Magnetecs-CGCI configurations seem superior to the other configurations considered. However, even in this special case, the results should be interpreted with caution. Those configurations allow the electromagnets to be placed substantially closer to the workspace than the other configurations considered, which is likely the primary reason for the positive result, but that comes at the cost of restricting access to the workspace. If the access could be equalized in some way (which would almost certainly be application specific), we may find that the benefits of the square-antiprism and Magnetecs-CGCI configurations are less pronounced. However, although having a large access solid angle may be important for some applications, utilizing multiple smaller access solid angles with a variety of approach vectors may be a better for other applications.

In our analysis, we chose to consider a fixed workspace size across configurations (i.e., a cubic workspace of side-length $0.5D_o$). As an alternative, we could have considered a workspace that scaled proportionally to the open volume between the electromagnets in each of the configurations. It is unclear how such a choice would have affected the results.

In our analysis, we only consider coreless (i.e., air-core) electromagnets, due to the relative simplicity that it affords. Most of the eight-electromagnetic systems in the literature utilize ferromagnetic cores, which could affect the generalizability of our results. However, we believe that it is unlikely to significantly affect our conclusions related to the relative comparisons between configurations, due to that fact that we found such an insensitivity to the geometry of the electromagnet considered. In addition, we only considered cylindrical electromagnets in our analysis. However, we recently conducted a study that revealed that cylinders (with the option of a tapered end at the innermost surface) are less than 1% weaker that the electromagnet of optimal geometry [15]. Finally, we constrained the axes of the electromagnets to all intersect at a common point at the center of the workspace; it is possible that this arbitrary constraint is suboptimal.

V. Conclusion

In the first contribution of this letter, we conducted a critical comparison of the manipulability of three eight-electromagnetic configurations that have appeared in the literature. We found that certain configurations are superior in terms of field and torque generation, whereas other are superior in terms of force generation (due to the spatial derivative in the field). In the second contribution of this letter, we propose a new open-asymmetric configuration that does not comprise the symmetry seen in prior systems yet still exhibits an isotropic workspace with comparable performance to prior systems, and that also provides more open access to the manipulation workspace than prior systems. Finally, we conclude that designers of isotropic eight-electromagnet manipulation systems should not feel obliged to incorporate symmetry into their design.

References

[1] E. Diller and M. Sitti, " Micro-scale mobile robotics," *Found. Trends Robot.*, vol. 2, no. 3, pp. 143–259, 2013.

[2] B. J. Nelson, I. K. Kaliakatsos, and J. J. Abbott, "Microrobots for minimally invasive medicine," *Annu. Rev. Biomed. Eng.*, vol. 12, no. 1, pp. 55–85, 2010.

[3] M. P. Kummer, J. J. Abbott, B. E. Kratochvil, R. Borer, A. Sengul, and B. J. Nelson, "OctoMag: An electromagnetic system for 5-DOF wireless micromanipulation," *IEEE Trans. Robot.*, vol. 26, no. 6, pp. 1006–1017, Dec. 2010.

[4] A. J. Petruska and B. J. Nelson, "Minimum bounds on the number of electromagnets required for remote magnetic manipulation," *IEEE Trans. Robot.*, vol. 31, no. 3, pp. 714–722, Jun. 2015.

[5] S. Erni, S. Schürle, A. Fakhraee, B. E. Kratochvil, and B. J. Nelson, "Comparison, optimization, and limitations of magnetic manipulation systems," *J. Micro-Bio Robot.*, vol. 8, no. 3, pp. 107–120, 2013.

[6] B. E. Kratochvil *et al.*, "MiniMag: A hemispherical electromagnetic system for 5-DOF wireless micromanipulation," in *Experimental Robotics*, (ser. Springer Tracts in Advanced Robotics). Berlin, Germany: Springer, 2014, pp. 317–329.

[7] E. D. Diller, "Remote actuation and control of multiple magnetic microrobots," Ph.D. dissertation, Dept. Mech. Eng., Carnegie Mellon Univ. Pittsburgh, PA, USA, 2013.

[8] E. Diller and M. Sitti, " Three dimensional programmable assembly by untethered magnetic robotic micro-grippers," *Adv. Functional Mater.*, vol. 24, no. 28, pp. 4397–4404, 2014.

[9] I. S. M. Khalil, V. Magdanz, S. Sanchez, O. G. Schmidt, and S. Misra, "Three-dimensional closed-loop control of self-propelled microjets," *Appl. Phys. Lett.*, vol. 103, 2013, Art. no. 172404.

[10] "Magnetecs CGCI." 2018. [Online]. Available: http://www.magnetecs.com/overview.php

[11] J. B. Brink, A. J. Petruska, D. E. Johnson, and J. J. Abbott, "Factors affecting the design of untethered magnetic haptic interfaces," in *Proc. IEEE Haptics Symp.*, 2014, pp. 107–114.

[12] J. Hua, C.-Y. Chang, N. Tardella, J. English, and J. Pratt, "Effectiveness of haptic feedback in open surgery simulation and training systems," *Stud. Health Technol. Inform.*, vol. 119, pp. 213–218, 2006.

[13] J. J. Thomson, "The structure of the atom: an investigation of the stability and periods of oscillation of a number of corpuscles arranged at equal intervals around the circumference of a circle; with application of the results to the theory of atomic structure," *London, Edinburgh, Dublin Philosoph. Mag. J. Sci.*, vol. 7, no. 39, pp. 237–265, 1904.

[14] J. Edelmann, A. J. Petruska, and B. J. Nelson, "Estimation-based control of a magnetic endoscope without device localization," *J. Med. Robot. Res.*, vol. 3, no. 1, 2018, Art. no. 1850002.

[15] J. J. Abbott and B. Osting, "Optimization of coreless electromagnets to maximize field generation for magnetic manipulation systems," *IEEE Magn. Lett.*, vol. 8, 2017, Art. no. 1300104.